



Contents lists available at ScienceDirect

Gondwana Research

journal homepage: www.elsevier.com/locate/gr

GR Focus Review

A review of numerical modeling studies of passive margin escarpments leading to a new analytical expression for the rate of escarpment migration velocity

Jean Braun*

ISTerre, Université Grenoble Alpes and CNRS, BP 53, Grenoble Cedex 9 38041, France

Helmholtz Centre Potsdam, German Research Center for Geosciences (GFZ), Telegrafenberg, Potsdam 14473, Germany

ARTICLE INFO

Article history:

Received 2 July 2016

Received in revised form 5 April 2017

Accepted 11 April 2017

Available online xxxx

Keywords:

Passive margin escarpments

Numerical modeling

Drainage divide migration velocity

Geomorphology

ABSTRACT

Passive margins are geomorphological features that have historically attracted much attention from the modeling community. In particular, many numerical modeling studies have attempted to explain the longevity of steep escarpments that formed along continental edges at the transition between low elevation coastal plains and high elevation continental interiors, such as along the coasts of Africa and South America on both sides of the South Atlantic Ocean. In this paper, I review the wide and diverse body of observational constraints gathered to constrain the formation and evolution of passive margin escarpments, as well as the various mechanisms that have been proposed to explain their anomalously high topography. I then compile and summarize the findings of numerous numerical modeling studies that have been performed in the past twenty years to explain their formation and evolution. I show that many of these studies converged to agree that the longevity of passive margin escarpments depends on how rapidly they become and remain regional drainage divides and that this is primarily controlled by the flexural isostatic rebound associated with the erosion of the high elevation continental interior. To better quantify these findings, I derive and present a new analytical expression for the migration velocity of an escarpment once it has become a drainage divide. This expression is validated by a series of numerical experiments using 1D and 2D high resolution landscape evolution models. Interestingly, these models also predict that the rate of erosion at or near escarpments can be several orders of magnitude smaller than the rate of escarpment retreat. This may explain the apparent discrepancy between the low estimates of present-day erosion rates obtained mostly from cosmogenic nuclide studies (10m/Myr) and the long-term rates of escarpment retreat (1km/Myr).

© 2017 International Association for Gondwana Research. Published by Elsevier B.V. All rights reserved.

Contents

1. Introduction	00
2. Observational constraints	00
3. The origin of the uplift	00
4. Past history of modeling	00
4.1. Key findings	00
4.2. Other important results	00
4.3. Outstanding issues	00
5. Drainage divide migration velocity	00
5.1. Balance between river incision and hillslope processes	00
5.2. Local Pe and divide migration	00
6. 1D numerical simulations	00
7. Escarpment retreat and effect of flexural isostasy	00
8. 2D numerical simulations	00
9. Future work	00

* Corresponding author at: Helmholtz Centre Potsdam, German Research Center for Geosciences (GFZ), Telegrafenberg, Potsdam 14473, Germany.
E-mail address: jbraun@gfz-potsdam.de.

10. Summary of findings	00
Acknowledgments	00
Appendix A. Supplementary data	00
References	00

1. Introduction

Many passive margins are characterized by a steep escarpment separating a low relief inland plateau from a higher relief coastal plain. Examples include the southeastern margin of Australia, the margins of Southern African, the margin of Brazil, Antarctica, Norway, Greenland and Newfoundland. Although there is been some controversy on the origin of this topography, i.e. whether it predates, is concomitant or postdates the rifting event that led to the formation of the margin, one of the most surprising characteristics of high elevation passive margins is their apparent longevity (Gilchrist and Summerfield, 1990). In many cases, and in particular, along the margins flanking the South Atlantic Ocean, the elevation of the margins is thought to be as old as the rifting event which took place in the Barremian-Aptian (Torsvik et al., 2009), some 130–115 Ma ago. The southern Brazilian and southwestern African passive margin escarpments are now locally situated several hundred kilometers from the coast. But they remain prominent, high relief features that have sustained over 100 Myr of erosion. This is principally why these features have been the focus of many modeling exercises. Some of the earliest models of landscape evolution (Gilchrist et al., 1994) were specifically designed to study passive margin escarpments and propose mechanisms to explain their longevity.

In this paper I first review the large body of observations concerning passive margin escarpments. I then rapidly list the mechanisms that have been proposed for their formation and review in details previous modeling studies. I then focus on the key issue of the processes that set the rate of drainage divide migration. Although I am mostly motivated by a need to understand the relative stability and slow evolution of passive margin escarpments, the work I present here may also be applicable to the dynamics of drainage divide migration elsewhere on Earth. I then derive a new expression for the migration velocity of a divide under the assumption that it is controlled by the balance between river incision and hillslope processes and show that, in the case of an escarpment, an asymptotic value exists that is only controlled by the rate coefficients of the assumed erosion process laws. I test this hypothesis using a simple 1D numerical solution of the stream power law coupled to a linear diffusion equation that is meant to represent hillslope processes. I then investigate how flexural isostasy may further control the rate of escarpment migration. All these concepts are then generalized to the 2D evolution of a passive margin escarpment by making use of a full planform numerical model of landscape evolution. Using this model, I also demonstrate that great caution must be taken in using erosion rate at or near the summit of an escarpment to estimate the rate of escarpment migration.

2. Observational constraints

In this section, I briefly review the existing observations that have been collected with the purpose of constraining the formation and evolution of high elevation escarpments that characterize many passive margins. I will focus on, but not limit myself to the margins flanking both sides of the south Atlantic Ocean, and, in particular, the southern margin of Brazil between Rio de Janeiro and Curitiba, and the southwestern African margin between Swakopmund in Namibia and Cape Town in South Africa. Both margin sections display prominent escarpments. In Fig. 1 I show a series of topographic profiles across sections of the southern African and Brazilian margins.

Both margins are characterized by a sharp escarpment separating a low topography, medium to high relief coastal plain from a high topography, low relief continental plateau. The plateau is approximately 800–1000 m high in both South Africa and Brazil. There is however some variability in the location of the escarpment and its expression in the landscape. Along profile B, for example, the escarpment is at the coast, whereas along profile F, it is more than 100 km inland. The relatively flat inland plateau is well defined along most profiles, except in profiles C and F. The escarpment is very steep along profiles A, B and F and is gently dipping towards the coastline along profile D. In all cases, the escarpment is a regional drainage divide.

The offshore sedimentary record has been used by many authors in an attempt to provide time and rate constraints on the erosion and retreat of passive margin escarpments. The common assumption is to equate the volume of sediment deposited offshore to the volume of material eroded during the inland migration of the escarpment. In many instances, the sedimentary record shows several pulses of sedimentation/erosion. For example, Gunnell and Fleitout (1998) combined offshore sedimentary data with onshore fission track data to constrain a model of passive margin escarpment evolution in the Western Ghats of India. More recently, Campanile et al. (2008) evidenced two major pulses of sedimentation in the Konkan-Kerala Basin, along the Western Indian passive margin, one in the Paleocene, corresponding to the major phase of rifting between India and the Seychelles, and a second one in the Pliocene that cannot be explained by simple escarpment retreat. Sugden and Denton (2004) used offshore sedimentary data from the Ross Sea to constrain the evolution of the Convoy Ranges in Antarctica. They concluded that most of the denudation along this passive margin occurred in the Eocene but that a second pulse of rapid erosion, potentially caused by the presence of fast flowing, wet-based glaciers, started around 30 Ma and lasted for approximately 15 Myr.

Peulvast et al. (2008) evidenced several phases of sedimentation in the offshore Ceará and Potiguar Basins of Brazil that postdate the opening of the central South Atlantic in the Aptian. The late Cretaceous rifting event is clearly observed in the sedimentary record as well as a Cenozoic event which Peulvast et al. (2008) interpreted as evidence for renewed uplift, erosion and flexural isostatic rebound of the continent edge.

Guillocheau et al. (2012) quantified the terrigenous flux along the Namibia-South Africa margin and showed that the Lower Cretaceous rifting is accompanied and followed by a period of intense sedimentation in the offshore Orange Basin. A second phase of sedimentation is observed in the late Cretaceous that lasted for approximately 30 Myr. Interestingly, the volume of sediment deposited during the first phase of erosion matches relatively well the amount of material removed from the coastal plain by propagation of the escarpment (Rouby et al., 2009), whereas the volume estimated for the second pulse of sedimentation in the late Cretaceous is estimated to be equivalent to up to 2.5 km of erosion over the entire present-day Orange River catchment (Guillocheau et al., 2012; Rouby et al., 2009). Similar pulses in erosion rate were recently confirmed by Wildman et al. (2015) using a large thermochronological dataset obtained from outcrop and borehole samples along the western margin of South Africa. They interpret the early Cretaceous (150–130 Ma) erosion phase to be related to rifting along the margin and the late Cretaceous (100–80 Ma) phase as the erosional response to a broader uplift potentially caused by mantle processes, which, locally, may have also led to the reactivation of basement structures (Wildman et al., 2016). This supports the suggestion of Braun et al. (2014a) that it is the tilting of the southern

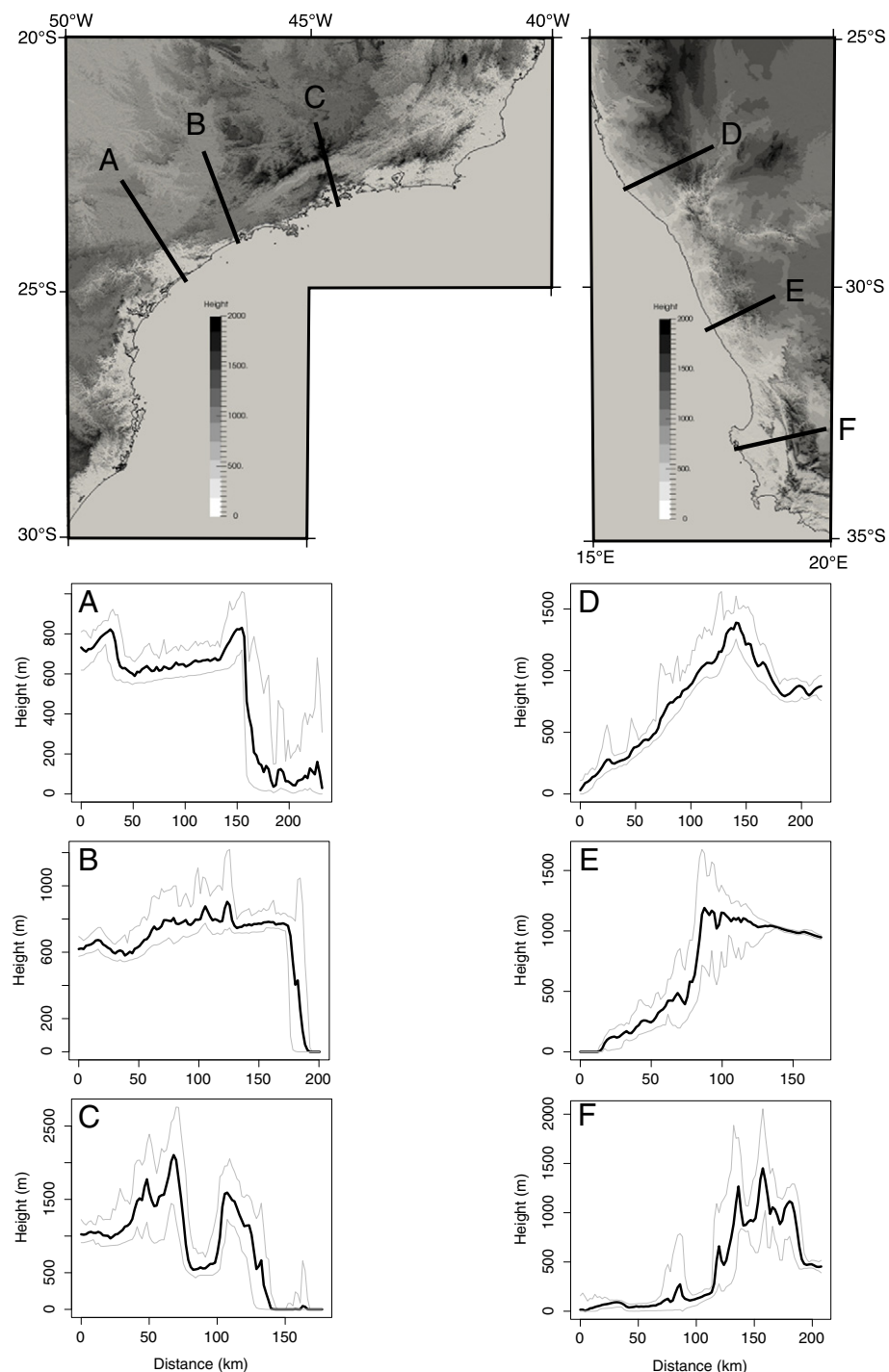


Fig. 1. Topographic maps of central Brazil (left) and southwestern Africa (right) including the location of 6 profiles shown in panels A to F (topographic data from global SRTM database). In each panel the mean topography (thick black line) across a 10 km wide swath along the profile, as well as the minimum and maximum elevations (grey lines) are shown.

African Plateau as it rode over a large mantle upwelling in the late Cretaceous that is responsible for that phase of widespread erosion. Wildman et al. (2015) note, however, that their data cannot be used to discard the possibility of a mild Cenozoic uplift phase that would have caused less than 1 km of erosion.

Steer (2012) compared offshore sedimentation in western Scandinavia with estimates of fjord erosion along the passive margin of Norway to show that substantial erosion must have taken place outside of the fjords, i.e. at high elevation, since the onset of northern hemisphere glaciations. Their interpretation suggests that the low

relief, high elevation surfaces observed along the Norwegian margin did not form at sea level, are relatively young and should, therefore, not be used as evidence for recent uplift of the margin as suggested by Lidmar-Bergstrom et al. (2000).

The processes by which passive margin escarpments evolve and retreat have been the subject of many investigations. Seidl et al. (1996) demonstrated that gorge head migration and the propagation of knickpoints along bedrock rivers that flow down the escarpment front are the main rate-setting processes acting along the southeastern margin of Australia. Weissel and Seidl (1997) demonstrated

from a detailed analysis of the link between bedrock jointing and the asymmetry of gorges that a strong coupling between fluvial and hill-slope processes is necessary to maintain headward propagation of gorge heads and is therefore likely to exert a strong control on the rate of drainage divide migration and escarpment retreat. Heimsath et al. (2006) demonstrated from cosmogenic nuclide data that there exists a strong linear decrease of erosion rate with elevation along the escarpment of southeastern Australia. They explained this rapid reduction in erosion rate from the base to the top of the escarpment as evidence for a strong control by stream incision and/or orographic precipitation.

There is ample evidence that the location, geometry and evolution of passive margins escarpments may be, in part, controlled by pre-existing lithological contrast and/or structures (Gunnell and Harbor, 2010; Weissel and Seidl, 1997). Most notable examples include the Drakensberg Mountain along the eastern margin of South Africa, the Blue Mountains of southeastern Australia, or the Western and Eastern Ghats of India. Van der Beek et al. (2002) showed that the more resistant Drakensberg Basalt must have played a key role in pinning the drainage divide atop the great escarpment of southeastern Africa. In Eastern Australia, the Hawkesbury Sandstone and the underlying units of the Narrabeen Group form a resistant layer on which part of the escarpment is built, especially in the Blue Mountain area (Van der Beek et al., 2001b). Gunnell and Harbor (2010) showed that the present-day geometry of the western Ghats escarpment in India is controlled by pre-existing structural weaknesses and lithological contrasts. They propose a simple model of escarpment evolution where the juxtaposition of strong and weak lithologies leads to the formation of embayments and detached "buttes".

Low-temperature thermochronological methods, such as fission track dating (AFT) or (U-Th)/He dating (AHE) in apatite, provides estimates of the cooling age of a rock, i.e. the time in the past when the rock cooled through a given, so-called closure temperature. These methods provide constraints on the rate and amount of erosion at the Earth's surface and have thus become essential tools in geomorphology. In Fig. 2, I show a non-exhaustive compilation of AFT ages for the passive margins of southern Brazil and southwestern Africa.

The Brazilian data is from Gallagher et al. (1994); the African data is from Brown et al. (1990). It is interesting to note that, along both margins, relatively few ages correspond to the rifting age (or range of ages). A marked difference however is the relative younging of the ages away from the coast and towards the escarpment in southwestern Africa, whereas in southern Brazil, this pattern is inverted with the youngest ages found near the present-day coastline. This suggests that, in Southern Africa, ages have been reset during the progressive retreat of the present-day escarpment and that such a retreat may have been most rapid in the few tens of millions of years that followed its inception during rifting (Brown et al., 1990). In Brazil, it is plausible that a more recent (i.e. post-rift) episode of uplift and erosion may have affected regions closest to the present-day coastline (Gallagher et al., 1994). Additional information can be derived from thermochronological datasets (making use of the relationship between age and elevation or depth down a borehole, the distribution of fission track lengths in AFT or the relationship between age and Uranium concentration in AHE), and used in complex inversion algorithms to deduce a cooling path rather than just a cooling age (see Wildman et al. (2016) for a good example of how these techniques have been used to constrain the evolution of a continental margin escarpment). However, despite these advances in data interpretation, the scenario and rate by which escarpments retreat are not well constrained. It remains uncertain whether escarpment migrate rapidly to their present day position soon after rifting or if their migration is slow and has progressed continuously since rifting (Braun and van der Beek, 2004). In situations where data density is high such as in the Drakensberg area along the east coast of South Africa (Brown et al., 2002), an alternate scenario has been proposed in which the escarpment main divide existed prior to rifting at a location very close to its present-day location (Van Der Beek et al., 2002). This would imply a very modest escarpment retreat rate that is consistent with present-day rates of retreat as measured by cosmogenic isotope methods.

Cosmogenic isotope analysis involves the measurement of the concentration of nuclides that have been produced by cosmic rays and have accumulated in the upper few meters of surface rocks.

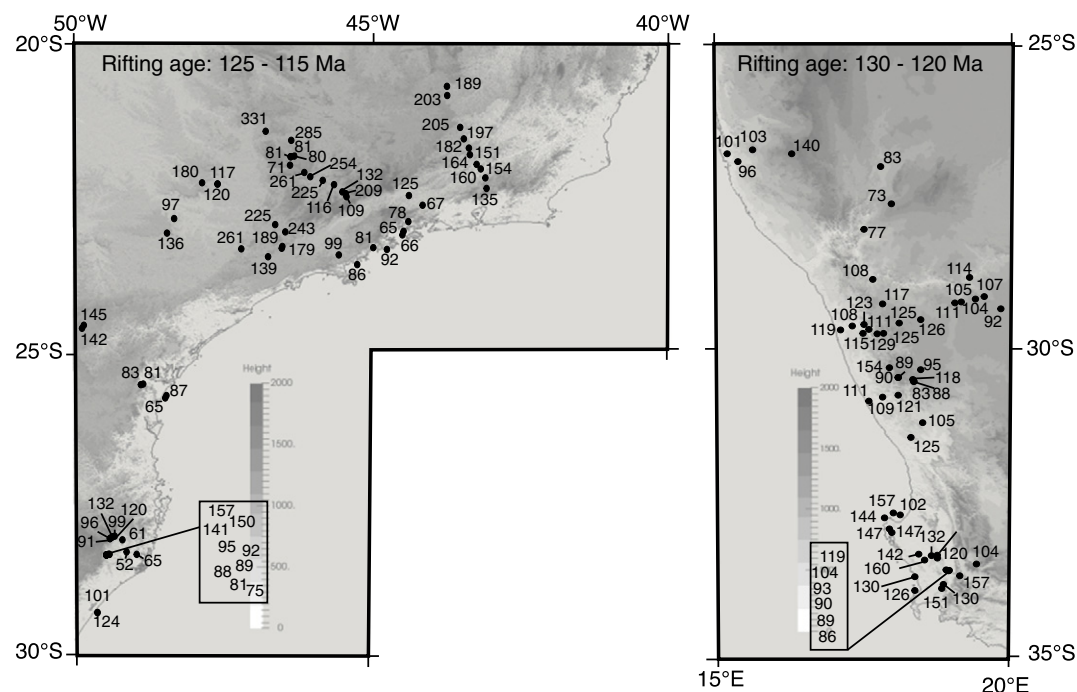


Fig. 2. Apatite fission track (AFT) ages for the central Brazilian and southwestern African margins. Ages in rectangular boxes correspond to age-elevation transects.

It provides means of assessing erosion rates over time scales of thousands to millions of years, either in situ or in river sediments. Combining in-situ cosmogenic analyses with AFT, Cockburn et al. (2000a) arrived at the conclusion that the present-day erosion rate at or near the great escarpment of Namibia is of the order of 10–20 m/Myr, which, combined with estimates derived from AFT data, implies a rate of escarpment retreat of only 10 m/Myr since the end of the Eocene. The present-day position of the escarpment implies an average retreat rate of 1 km/Myr which requires that the rate of escarpment retreat was much higher following break-up. Fleming et al. (1999) were in fact the first to document low escarpment retreat rates (50–100 m/Myr) but from the Drakensberg area along the southeastern margin of Africa. Other parts of the escarpment flanking the South African Plateau display similar low erosion rates (Kounov et al., 2007). Heimsath et al. (2006) reports similar results from the escarpment of southeastern Australia where measured present-day erosion rates at the escarpment are relatively small (of the order of a few m/Myr), suggesting that the escarpment is relatively stable. This also implies that the rate of escarpment retreat must have been much larger at breakup time to explain its present-day position (approximately 50 km from the present-day coastline, 100 Myr after breakup). Using river samples, Vanacker et al. (2007) documented faster cosmogenic nuclide derived erosion rates (20–70 m/Myr) along the flanks of the southern escarpment of Sri Lanka in comparison with the adjacent high elevation plateau above it and the lowland areas beneath it (2–6 m/Myr). They concluded, however, that, despite the relatively high erosion rate along the face of the escarpment, the cosmogenic-isotope data suggest a reduction in escarpment retreat rate in the recent past. A similar study was conducted by Mandal et al. (2015) along the western Ghat in southern India that reached very similar conclusions about the asymmetry in the present-day erosion rate between the escarpment (\approx 100 m/Myr) and the adjacent plateau (\approx 10 m/Myr) and its implication for the stability of the escarpment. In general, cosmogenic nuclide-derived rates support the idea that passive margin escarpments are relatively stable geomorphic features (Matmon et al., 2002). Similar low escarpment retreat rates have been confirmed by $^{40}\text{Ar}/^{39}\text{Ar}$ dating of K-Mn oxides (Beauvais et al., 2016).

3. The origin of the uplift

Many reasons have been proposed to explain the presence of high topographic features along passive margin escarpments. Most have in common that they seek to produce a long-lasting uplift, i.e. that survives the rifting process by many tens to hundreds of millions of years. These include the existence of substantial, pre-rift topography, usually in the form of a continental plateau; flexure of the continental lithosphere associated with the rifting process and the thinning of the lithosphere/crust leading to uplift of rift shoulders (Braun and Beaumont, 1989; Weissel and Karner, 1989); depth-dependent necking (Royden and Keen, 1980); asymmetric extension (Lister et al., 1991); secondary convection in the asthenosphere and/or upper mantle driven by the strong lateral contrast in lithospheric thickness across a nascent passive margin (Buck, 1986; Keen, 1985); or thermal expansion associated with lateral conduction of the heat anomaly generated during rifting (Cochran, 1983).

Several authors have, however, argued that some if not most of the present-day topography observed along elevated passive margins is young, i.e. younger than the time of continental rifting that led to the formation of the margin. The mechanisms that could lead to such rejuvenation of the topography remain poorly known and/or debated. It may be caused by the propagation of compressional in-plane stresses from far-away tectonically active regions (Japsen et al., 2012) or by areas of active mantle flow causing dynamic topography (Walford and White, 2005).

4. Past history of modeling

A major advance has helped revolutionized the way we study landscape evolution (Summerfield, 2005) and in particular the geomorphic evolution of passive margins: the development and use of numerical models that have bridged the gap between our understanding of local scale processes and large-scale conceptual models of landscape evolution (Summerfield, 2005).

4.1. Key findings

Earliest models of landscape evolution at passive margins involved computing the flexural isostatic response of an imposed erosional load (Gilchrist and Summerfield, 1990) to show that their persistence through geological time is most likely related to the amplitude of this isostatic response which determines whether escarpments become and remain drainage divides, a view that remains shared by most geomorphologists today. Soon followed a flurry of studies (Gilchrist et al., 1994; Kooi and Beaumont, 1994; Tucker and Slingerland, 1994) that attempted to reproduce the geometry of passive margin escarpments based on newly developed LEMs (or landscape evolution models). These models differ in the form of the equations being solved to represent surface processes, as well as in the methods used to solve them. Most models, however, represent surface processes as a combination of several types of processes which are referred to by Kooi and Beaumont (1994) as diffusion, reaction and advection and represent, according to Tucker and Slingerland (1994), hillslope processes, i.e. slope driven transport of weathered material on hillslopes, incision within bedrock channels that transforms bedrocks into suspended sediment load, and entrainment and transport of sediment in alluvial channels, respectively. Most models include flexural isostasy, i.e. the laterally distributed isostatic rebound associated with erosion and sedimentation at the Earth's surface (Gilchrist et al., 1994; Kooi and Beaumont, 1994; Tucker and Slingerland, 1994).

Using these models many researchers have attempted to address some of the key questions regarding the formation and evolution of passive margin escarpments, i.e. whether they are the product of a localized drop in base level at the coast during the rifting event or the product of a gentler, longer wavelength, up-warping of the surface; whether they propagate towards their present-day, more inland positions, by escarpment retreat or whether they form along a pre-existing inland drainage divide; whether, following rifting, they rapidly evolve to their present-day position and remain relatively stable thereafter, or whether they steadily migrate inland at a much slower pace; how important are lithological contrasts, climate variability, orographic control on precipitation or local stream capture as controlling factors on the rate and nature of escarpment evolution. Key findings included the following:

- the formation and stability of an escarpment depends strongly on whether it is a drainage divide or not; this is a direct consequence of the assumption that drainage area is a key controlling parameter for bedrock channel incision;
- slow escarpment retreat is the most likely evolution scenario once the escarpment is the main drainage divide;
- escarpment retreat stops when inland catchment areas are captured and leads to the formation of isolated topographic highs in the coastal plains from the remnants of a previous escarpment;
- pre-existing drainage divides as well as the existence of an elevated plateau in the continental interior control the rate of evolution and final position of passive margin escarpments;
- the rate of escarpment retreat and evolution is primarily set by the fluvial erosion parameter/constant but the competition between advective and diffusive processes determines the shape (sharp versus convex up escarpment top), rate of evolution and stability of escarpments;

- flexural isostasy is a main factor controlling whether escarpment are or become major drainage divides and low flexural rigidity (small flexural wavelength) promotes escarpment stability and reduces their rate of inland propagation; and
- lithological contrasts are important in determining the exact shape of the escarpment scarp but are not necessary to create and maintain the escarpment over geological time scales.

In Fig. 3 I show the results of eight *FastScape* model runs that illustrate these key findings. The reader is referred to Braun and Willett (2013) for a detailed description of this landscape evolution model, which I also describe in the later part of this manuscript. I provide, as supplementary material, animations of all model runs to help the reader appreciate the dynamic evolution of the escarpment under the various assumptions. I also provide the input files that were used to perform each of the runs with *FastScape*, which can be obtained from the author.

4.2. Other important results

Van der Beek and Andriessen (1995) were the first to combine numerical modeling with thermochronological constraints to estimate the timing of uplift and erosion. Combining a simple 1D SPM with a more complex tectonic model for the syn-rift formation of rift shoulders and the post-rift thermal subsidence of the margin, they attempted to reproduce fission track ages and length pattern distributions observed along several passive margins. They concluded that syn-extension uplift and subsequent erosion of the rift flank can explain most of the thermochronological data but that ages that are substantially younger than the rifting age require rejuvenation of the topography by a later tectonic event. Similar studies followed that combined numerical modeling and thermochronological constraints to study the evolution of rifted margin escarpments, such as Gunnell and Fleitout (1998) in the Western Ghats in India, or Cockburn et al. (2000b) along the Namibian sector of the south-west African margin. By coupling an SPM to a full 3D thermo-kinematic model, Braun and van der Beek (2004) demonstrated, however, that the thermochronological record at passive margins is unlikely to provide definite constraints on the rate of propagation of escarpments. This is because the total amount of erosion associated with the retreat of an escarpment, i.e. less than a couple of kilometers, is unlikely to reset isotopic and fission track systems characterized by a closure temperature of 70–120 °C. Borehole data are very useful in resolving this uncertainty as demonstrated by Van Der Beek et al. (2002), but several important parameters of the coupled mechanical/thermal/erosional system remain very difficult to constrain, such as the temperature gradient during and following rifting, the lithospheric flexural strength and its evolution through time, as well as the basic erosional parameters, such as the fluvial erosion constant and the hillslope transport coefficient.

Van Balen et al. (1995) used a similar approach to Van der Beek and Andriessen (1995) to predict the geometry of the sedimentary wedge deposited offshore of an uplifted rift flank. They predicted the formation of an initial offlapping sequence resulting from the rapid influx of sediment from the eroding rift shoulder and the concomitant isostatic rebound, followed by a longer lasting (often still ongoing) onlapping sequence that is mostly controlled by the thermal subsidence of the margin as well as the reduced sediment supply from the decaying continental topography.

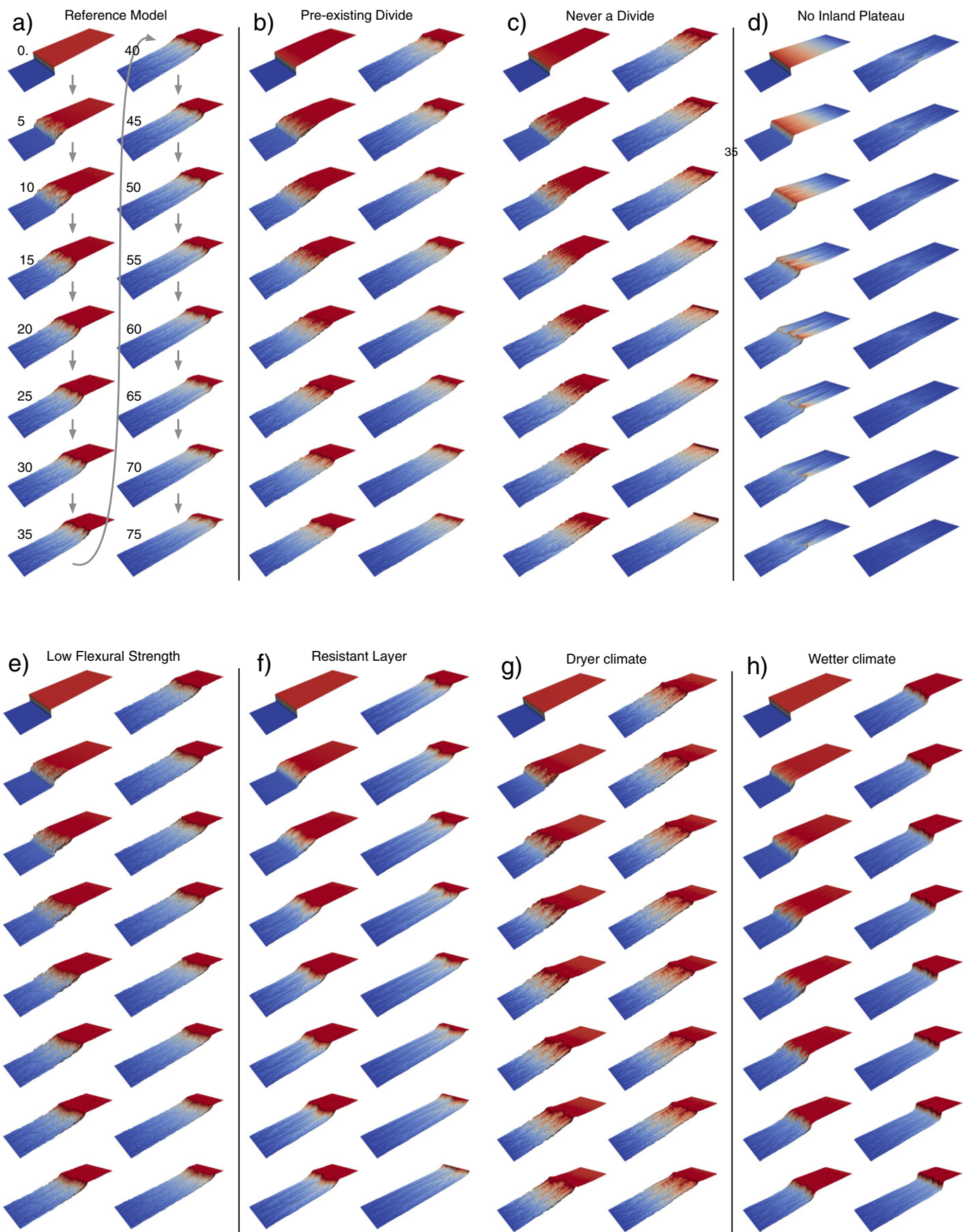
Combining a detailed morphometric analysis with estimates of erosion rate derived from cosmogenic data, Weissel and Seidl (1998) showed that fluvial erosion by the propagation of knickpoints is one of the major processes controlling escarpment retreat rate. They were also among the first to recognize that the very existence of knickpoints implies that the slope exponent in the bedrock incision law must be larger than or equal to one. Van der Beek and Braun (1998) conducted a more thorough investigation of how the parameters of LEMs can be constrained by comparing geomorphic characteristics between natural and modeled landscapes, focusing on the highlands and passive margin escarpment of southeastern Australia. Their main conclusion is that the rate defining parameters cannot be constrained from the form of the landscape alone and that the inclusion of diffusion (hillslope processes) in the LEMs is contingent on achieving a sufficient spatial resolution (i.e. less than 1 km). By noting this, they thus highlighted the main shortcoming of many LEMs, which, on the one hand, claimed to be able to connect the small scale processes to the long-term evolution of a landform but, on the other hand, were limited by computational efficiency to spatial resolutions much coarser than the scale at which the local processes had been evidenced, parameterized and, in some cases, calibrated.

Several important studies tested the main ideas put forward for the formation and evolution of passive margins escarpments by applying numerical models to specific case studies. These included Van der Beek et al. (1999) and Van der Beek and Braun (1999) for the Southeastern Highlands of Australia and the adjacent uplifted margin of the Tasman Sea, Van der Beek et al. (2001a) for the Blue Mountains of Southeast Australia, Van Der Beek et al. (2002) for the Drakensberg escarpment of southeastern Africa, and Petit et al. (2007) for the Dhofar passive margin flanking the northern coast of the Gulf of Aden in Oman.

More recently, Sacek et al. (2012) demonstrated that a secondary flexural bulge created by flexure during rifting and extension can become an inland drainage divide that serves to pin the escarpment during its retreat or cause a double escarpment geometry to develop as observed along the Serra do Mar section of the southeastern Brazilian margin and parts of the southeastern Australian margin. This modeling result suggests that the presence of an inland drainage divide is not necessarily the result of a pre-rift topographic pre-conditioning but can arise from the rifting process itself.

Braun et al. (2012) coupled a simplified surface processes model with a 3D, temperature dependent flexural model of the lithosphere

Fig. 3. Results of 8 model runs using the *FastScape* model illustrating the key findings of previous modeling studies. a) Reference model. Dimensions are 150 × 50 km. Discretization is 300 × 100 points. 750 times steps of 10⁵ year duration were used but solution is shown every 5 Myr only in the direction indicated by the arrows; numbers indicate model time in Myr. The model solves the stream power law that relates erosion rate by rivers to slope and drainage area to the power $m = 0.4$; constant of proportionality is $K_F = 5 \times 10^{-6} \text{ m}^{1-2m}/\text{yr}$. It also solves the diffusion equation representing hillslope processes with a diffusivity (or transport coefficient) of $K_D = 0.14 \text{ m}^2/\text{yr}$. The model also solves the flexural isostasy equation with an effective elastic plate thickness of 20 km. Boundary conditions are fixed height at the boundaries furthest away from each other and cyclic boundary conditions at the two others. No uplift is imposed in addition to the flexural isostatic rebound. Initial topography is a 1000 m high plateau that initially occupies three-quarter of the model, as shown at time step 1 in panel a. The model results show that, due to the flexural response, the escarpment rapidly becomes the main drainage divide. This slows down its evolution and leads to the retreat of the escarpment towards the continental side of the model at a relatively slow pace (approximately 1 km/Myr). b) The presence of a pre-existing drainage divide inland of the escarpment leads to the disappearance of the escarpment until erosion abuts against the divide and the escarpment is re-created ($t = 0$ to $t = 30$ Myr); it then resumes its migration at the same pace as in the reference model. c) If the continental interior dips towards the coast such that the escarpment never becomes a divide, the initial escarpment rapidly disappears and the initial plateau is eroded away (in about 30 Myr). d) If there is no inland plateau, the rift shoulder uplift is rapidly eroded away; note also that the escarpment is always the main divide and does not propagate inland with time. e) Decreasing the effective elastic plate thickness (from 20 to 5 km) reduces the flexural isostatic wavelength; the escarpment is not only better defined, but also it is characterized by steeper sides and migrates at a reduced rate towards the continental interior. f) The presence of a 500 m thick resistant layer increases the slope on the seaward side of the escarpment but does not really affect its rate of retreat. g) Decreasing or h) increasing the river incision efficiency coefficient, K_F , slows down or accelerates the escarpment retreat. Changing K_F can be regarded as changing the mean precipitation rate.



to show how the three-dimensionality of a rift, and, in particular, the existence of transform sections, strongly controls the distribution of flexural uplift and subsidence. Such an amplification of flexural uplift and subsidence is observed, they argue, along parts of the Western Africa Transform Margin.

4.3. Outstanding issues

Although much has been gained by simulating passive margin escarpment evolution using early numerical models of landscape evolution, some fundamental questions remain. The first question is what controls the velocity at which an escarpment, and, more generally, a drainage divide propagates. Models have shown that it is somehow related to the rate constants in the advection (stream power law) and diffusion (hillslope processes) terms of the basic equation, but the exact nature of this relationship is still to be determined. The second question is why flexure, and, in particular, the effective elastic thickness (EET) of the lithosphere, controls the rate of propagation of the escarpment: the smaller the EET, the slower the escarpment retreat.

5. Drainage divide migration velocity

5.1. Balance between river incision and hillslope processes

According to the stream power law, the rate of stream or fluvial incision is proportional to slope, S and drainage area, A :

$$\frac{\partial h}{\partial t} = -K_F A^m S^n = -K_F A^m \left(\frac{\partial h}{\partial x} \right)^n \quad (1)$$

The exponents m and n are poorly constrained but their ratio is often assumed to be close to 0.4. For simplicity here, I will use $n = 1$ and $m = 0.4$. Making use of Hack's law, which relates drainage area to distance to the divide:

$$A = k(L - x)^p \quad (2)$$

where $L - x$ is the distance from the divide situated at a distance L from a fixed base level, one can recast the stream power law in the following way:

$$\frac{\partial h}{\partial t} = -K_F k^m (L - x)^{mp} \frac{\partial h}{\partial x} \quad (3)$$

Near the divide, river incision and hillslope processes compete to set the rate of landscape evolution. I will use the simplest formulation to represent hillslope processes, making the assumption that the flux of material is linearly proportional to local slope. The processes that are included in such a representation are numerous and active over a range of scales. They may include soil creep, landsliding, rainsplash, overland transport, and periglacial processes. Assuming mass conservation, this yields the following expression for the rate of change of topographic height by hillslope processes:

$$\frac{\partial h}{\partial t} = K_D \frac{\partial^2 h}{\partial x^2} \quad (4)$$

where K_D is a transport coefficient or diffusivity. Combined with the stream power law, this yields the general equation describing the balance between the two processes that set the rate of landscape evolution near divides:

$$\frac{\partial h}{\partial t} = -K_F k^m (L - x)^{mp} \frac{\partial h}{\partial x} + K_D \frac{\partial^2 h}{\partial x^2} \quad (5)$$

Introducing the following dimensionless variables and unknowns:

$$h' = h/h_0, \quad x' = x/L \quad \text{and} \quad t' = t/\tau \quad (6)$$

yields

$$\frac{h_0}{\tau} \frac{\partial h'}{\partial t'} = -K_F k^m L^{mp} (1 - x')^{mp} \frac{h_0}{L} \frac{\partial h'}{\partial x'} + K_D \frac{h_0}{L^2} \frac{\partial^2 h'}{\partial x'^2} \quad (7)$$

where h_0 is the height of the divide and τ a characteristic time scale. Using the diffusive time scale:

$$\tau_D = \frac{L^2}{K_D} \quad (8)$$

as reference or characteristic time scale, one obtains the dimensionless form of the same equation:

$$\frac{\partial h'}{\partial t'} = -Pe \frac{\partial h'}{\partial x'} + \frac{\partial^2 h'}{\partial x'^2} \quad (9)$$

where

$$Pe = \frac{K_F k^m L^{mp+1}}{K_D} \quad (10)$$

is the Peclet number (see Perron et al. (2008) for a similar derivation of the geomorphic Peclet number).

The Peclet number is a measure of the relative efficiency of fluvial vs. hillslope processes at setting the pace of landscape evolution (Perron et al., 2008). It can also be regarded as the ratio of two time scales:

$$Pe = \tau_D/\tau_F \quad (11)$$

where τ_F is the river incision time scale:

$$\tau_F = K_F k^m L^{mp-1} \quad (12)$$

These expressions tell us that the rate of evolution of the landscape will be mostly dictated by the length L , as well as geometrical constants, k and p , and parameters, K_D , K_F and m , that are functions of lithology and climate (mean rainfall). One must remember, however, that the stream power law and the linear diffusion equation are only first-order parameterizations of the true processes controlling river incision and hillslope processes. The parameters K_D , K_F and m are likely to be functions of rainfall and/or discharge variability, fracturing, vegetation cover and type, soil thickness and its rate of evolution, for example.

5.2. Local Pe and divide migration

As proposed by Perron et al. (2008), one can introduce a characteristic length scale, L_E , for which the Peclet number is unity. Points that are located at such a distance from a water divide are equally affected by hillslope processes (diffusion) and river incision. From the definition of the Peclet number (Eq. (10)), one can derive the following expression for L_E :

$$L_E = \left(\frac{K_D}{K_F k^m} \right)^{\frac{1}{mp+1}} \quad (13)$$

The rate of propagation of the divide must be related to the difference in erosion rate scaled by the relative slopes on either sides of the divide, S_1 and S_2 :

$$v_d \propto \frac{\frac{\partial h}{\partial t}|_1 - \frac{\partial h}{\partial t}|_2}{S_1 + S_2} \quad (14)$$

This relation assumes that topography in the vicinity of the divide can be approximated by two oppositely dipping planes. I will make the assumption that the erosion rates and slopes in this expression can be estimated at a distance close to L_E to provide meaningful values for the divide migration rate. At a distance L_E from the divide, the rate of erosion by river incision and diffusive transport are similar and must be equal to

$$\frac{\partial h}{\partial t} = K_F A_E^m S_E \quad (15)$$

where A_E and S_E are the drainage area and slope at a distance L_E from the divide. From this I can derive the following expression for the divide migration velocity:

$$v_d = 2K_F A_E^m \frac{S_{1E} - S_{2E}}{S_{1E} + S_{2E}} \quad (16)$$

The factor 2 comes from the fact that river incision only account for half the erosion rate at a distance L_E from the divide. From the definition of L_E and making use of Hack's Law, we can finally write

$$v_d = 2(K_F k^m)^{\frac{1}{mp+1}} K_D^{\frac{mp}{mp+1}} \frac{S_{1E} - S_{2E}}{S_{1E} + S_{2E}} \quad (17)$$

This expression gives the rate of divide migration as a function of the erosional parameters K_F , K_D and m (assuming $n = 1$), Hack's Law coefficients (k and p) and local measures of slopes at a relevant distance on either side of the divide. We will see that it can later be simplified in the case of an escarpment.

The relevant distance is the characteristic length, L_E , beyond which river incision is expected to dominate over diffusion. A commonly used method to determine the part(s) of a landscape where river incision dominates (and the stream power law governs incision) is to consider the relationship between surface slope and drainage area. Under the assumption that a river profile has reached steady state between uplift and incision, one can write

$$\frac{\partial h}{\partial t} = 0 = U - K_F A^m S^n \quad (18)$$

which implies that along a steady-state river profile there must exist a linear relationship between the logarithm of drainage area and the logarithm of slope (Willgoose et al., 1991):

$$\log S = \log k_{sn} - \theta \log A \quad (19)$$

where,

$$k_{sn} = \left(\frac{U}{K_F} \right)^{1/n} \quad (20)$$

is channel steepness, and

$$\theta = m/n \quad (21)$$

is concavity index. Many studies have been performed in a wide variety of environments (Montgomery, 2001; Willgoose et al., 1991) that show that the area for which this relationship breaks down is in the

range 10^4 – 10^5 m², indicating that the critical length scale from the divide for the transition from river incision (stream power law) to hillslope processes must be of the order of $L_E = 100$ – 300 m.

6. 1D numerical simulations

To test whether this scaling argument holds, I have designed a simple numerical scheme to solve the landscape evolution equation (Eq. (5)) combining river incision and hillslope processes. I used a centered finite difference scheme for the second order derivative in the term representing the hillslope processes and a forward finite difference scheme (in the direction of the slope) for the first order derivative in the term representing river incision. I used an implicit time integration scheme that leads to a tri-diagonal system of equation, which I solve by Gaussian elimination. The drainage area is computed by using Hack's law.

In Fig. 4a, I show the solution in terms of computed topographic profiles at time intervals of 1 Myr for 10 Myr, from an initial triangular hill shown as the dashed line, i.e. an asymmetric ridge with

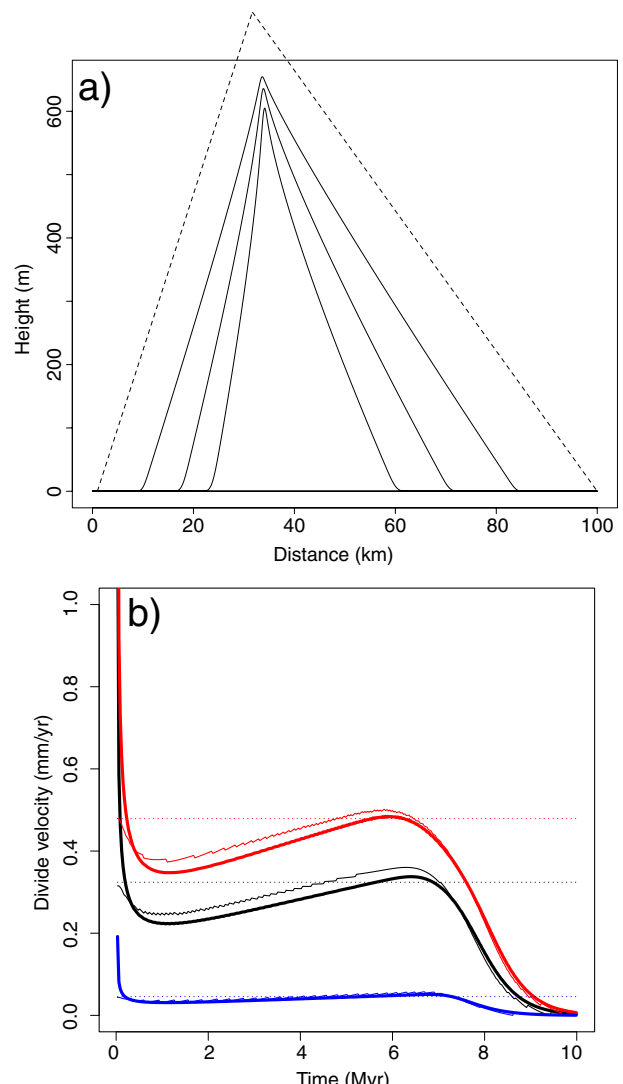


Fig. 4. a) Computed topographic profile solutions of Eq. (5). See text for parameter values. Dashed line is initial topography. Note the very large vertical exaggeration (1000×). b) Computed divide velocity (thick solid line) and velocity derived from Eq. (17) (thin solid line). The thin dotted line is the velocity estimated from the initial topography. The black lines correspond to $S_R = 2$; the red lines to $S_R = 3$, and the blue lines to $S_R = 1.1$.

straight sides. The model length is 100 km which is discretized at a resolution of 10 m; the time step length is 100 yr; $m = 0.4$; $p = 5/3$; $k = 6.7 \text{ m}^{2-p}$; $K_F = 5 \times 10^{-6} \text{ m}^{1-2m}/\text{yr}$ and $K_D = 0.14 \text{ m}^2/\text{yr}$ such that $L_E = 300 \text{ m}$. The asymmetry of the system is controlled by the relative slope of the initial profile on the lefthand side of the divide, S_R , compared to the righthand side.

Through time the hill gets narrower, smaller and slightly steeper; its sides evolve to develop a curvature (or concavity) typical of river profiles. The summit is rounded and characterized by a negative, finite curvature. I computed the position of the divide, x_d , at each time step and its velocity by simple finite difference:

$$v \approx \frac{x_d(t + \Delta t) - x_d(t)}{\Delta t} \quad (22)$$

This velocity is shown as the thick black curve in Fig. 4b. The velocity obtained from Eq. (17), v_d , is also shown as the thin black curve and agrees very well with the observed velocity. The dotted lines correspond to the velocity obtained by using the initial topographic slopes to estimate the velocity. The solution was also computed for different degree of initial topographic asymmetry (S_R) and the results are shown in Fig. 4b too. We see that, in all cases, the divide velocity is initially very large but rapidly decreases to reach a near steady state value. It then increases slowly until approximately 6 Myr into the evolution of the run where it rapidly decreases towards zero. The first phase of rapid velocity decrease corresponds to the evolution of the system towards a quasi-steady state shape that later evolves mostly by its amplitude. During the second phase the slow, steady increase in velocity corresponds to an increase in the slope difference across the divide. The transition between the latter two regimes (where the velocity rapidly evolves to zero) takes place when the hill has become sufficiently small that its size is of the order of L_E .

In Fig. 5 I show the computed velocity for 5 different runs, corresponding to different combinations of three different values of K_F and K_D . The black curves are identical to those shown in Fig. 4b for reference. The blue curves are those corresponding to a larger K_D , keeping K_F constant, which leads to a faster divide migration. The red curves correspond to a smaller value of K_D , keeping K_F constant, which leads to smaller divide migration velocities. The green

and orange curves correspond to smaller and greater values of K_F , respectively, but adjusting K_D such that the length scale L_E remains constant at 300 m. Smaller/larger K_F values leads to slower/faster divide migration velocities, respectively. In all cases, the predictions of the model agree with the value derived by assuming that the rate of divide migration is set by the difference in erosion rate on either side of the drainage divide at a distance equal to L_E .

7. Escarpment retreat and effect of flexural isostasy

By definition, an escarpment is a geomorphic feature that is characterized by an extreme asymmetry in slope. The top of an escarpment is a drainage divide that separates a region of almost infinite slope from a region of almost zero slope. In this situation, the Eq. (17) governing the divide migration velocity becomes

$$v_d = \lim_{S_{1E} \gg S_{2E}} 2(K_F k^m)^{\frac{1}{mp+1}} K_D^{\frac{mp}{mp+1}} \frac{S_{1E} - S_{2E}}{S_{1E} + S_{2E}} = 2(K_F k^m)^{\frac{1}{mp+1}} K_D^{\frac{mp}{mp+1}} \quad (23)$$

This expression is independent of the shape of the escarpment, as long as it is characterized by a strongly asymmetric geometry. We will call it the escarpment “intrinsic” migration velocity.

In Fig. 6 are shown results of computations similar to those shown in Fig. 4b but in which the initial topography is a 1000 m high vertical escarpment on which a small, 100 m high triangular taper has been added on the upper side of the escarpment to make sure that it is and remains a drainage divide. The solution is computed over a domain that is 2000 km long at a resolution of 100 m. In Fig. 6, we see that after a short transient period of rapid decrease, the velocity of escarpment migration reaches a quasi steady-state value that slowly converges towards the theoretical, intrinsic value given by Eq. (23). This is confirmed by a series of runs in which the model parameters (K_F , L_E and K_D) have been varied (Fig. 6). In all cases, the velocity of the escarpment is relatively uniform and tends towards the intrinsic value.

To estimate the effect of flexural isostasy on the velocity of divide migration at a passive margin escarpment, I coupled the landscape

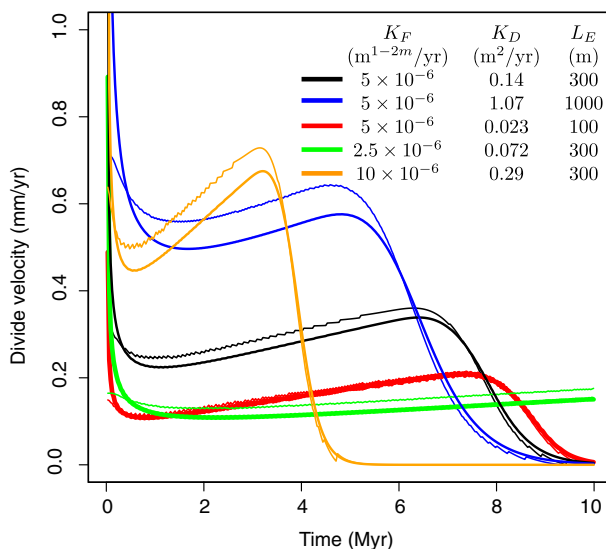


Fig. 5. Computed divide velocity (thick line) and obtained from Eq. (17) (thin line). The different colors correspond to various values of the erosional parameters, K_F and K_D , as given in the legend.

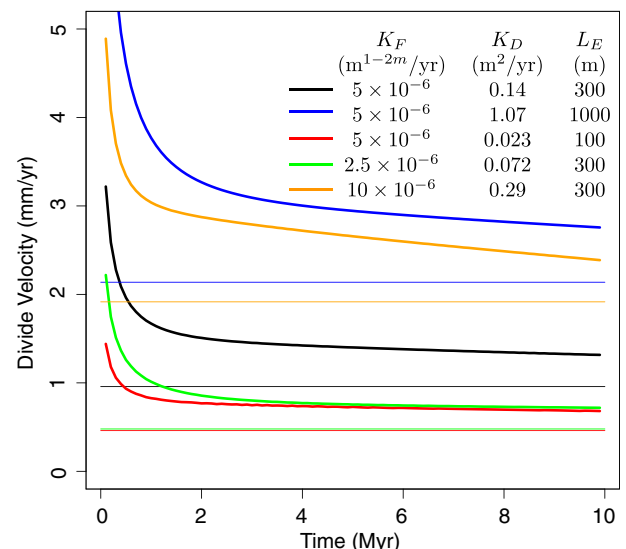


Fig. 6. Computed escarpment divide velocity (thick line) and obtained from Eq. (23) (thin line). The different colors correspond to various values of the erosional parameters, K_F and K_D , as given in the legend.

evolution equation (Eq. (5)) to the following equation for the flexural isostatic rebound, Δu resulting from an erosional increment, Δh :

$$D \frac{\partial^4 \Delta u}{\partial x^4} = \Delta \rho g \Delta u + \rho_s g \Delta h \quad (24)$$

where

$$D = \frac{ET_e^3}{12(1-\nu^2)} \quad (25)$$

E is Young Modulus, ν is Poisson's ratio, T_e is the effective elastic thickness (EET) of the lithosphere, $\Delta \rho$ the density difference between asthenospheric rock density, ρ_a , and surface rock density, ρ_s , and g is gravitational acceleration. I solved the flexural isostasy equation using the spectral method described in Nunn and Aires (1988) and an FFT method (Press et al., 1992) over $10^{12} = 8192$ points.

The evolution of surface topography was computed over the same domain ($L = 2000$ km), discretized at a 100 m resolution. As in the previous runs, the initial topography was set to be a 1000 m tall plateau over half the domain size to which a small 100 m tall and 1000 km wide triangular wedge was added. I used the same erosional constant as for the reference run shown in Fig. 4, namely $K_F = 5 \times 10^{-6} \text{ m}^{1-2m}/\text{yr}$, $K_D = 0.14 \text{ m}^2/\text{yr}$ and $m = 0.4$ such that $L_E = 300$ m. I also used $E = 1 \times 10^{11} \text{ Pa}$, $\nu = 0.25$, $\rho_s = 2800 \text{ kg/m}^3$, $\rho_a = 3150 \text{ kg/m}^3$ and $g = 9.81 \text{ m/s}^2$. The time step is 200 yr. The computed topography is shown in Fig. 7 at 1 Myr intervals.

As seen in Fig. 7a, the computed topography shows the effect of the flexural isostatic rebound as an amplification of the escarpment height over a wavelength ≈ 100 km, which is approximately 5 times the EET, as predicted by flexure theory (Turcotte and Schubert, 1982). The escarpment (or divide) migration velocity is a strong function of the assumed EET, as shown in Fig. 7b. Decreasing the EET causes the escarpment migration velocity to decrease. For very large values of the EET ($T_e = 100$ km), the escarpment migration velocity tends towards the intrinsic velocity, v_d . In this case, the evolution of the escarpment is nearly identical to that predicted without isostasy. When the EET is decreased towards more realistic values for a passive margin escarpment (EET = 20 or 5 km), the computed escarpment migration velocity tends towards values that are smaller than v_d , i.e. the escarpment is a more stable geomorphic feature. For unrealistically small values of the EET (1 km or 100 m), the escarpment velocity tends towards approximately 1/10th of the intrinsic velocity v_d .

These results can easily be understood if one considers that, when isostasy is taken into account, the rate of surface topography change, $\partial h / \partial t$ is not only controlled by the rate of erosion, $\partial E / \partial t$ but also by the rate of isostatic rebound, according to

$$\frac{\partial h}{\partial t} = \frac{\partial h}{\partial E} \frac{\partial E}{\partial t} \quad (26)$$

where $\partial h / \partial E$ is the rate of isostatic rebound per unit erosion, which is given by

$$\frac{\partial h}{\partial E} = 1 - \frac{\rho_s}{\rho_a + \frac{D}{g}(\frac{\pi}{W})^4} \quad (27)$$

where W is the width of the topographic feature being eroded, as shown in Braun et al. (2014b). Because the rate of escarpment/divide migration is directly proportional to the rate of topographic change, this leads to a new expression for the intrinsic migration velocity of escarpments that takes into account the effect of flexural isostasy:

$$v_d = 2(K_F k^m)^{\frac{1}{mp+1}} K_D^{\frac{mp}{mp+1}} \left(1 - \frac{\rho_s}{\rho_a + \frac{D}{g}(\frac{\pi}{W})^4} \right) \quad (28)$$

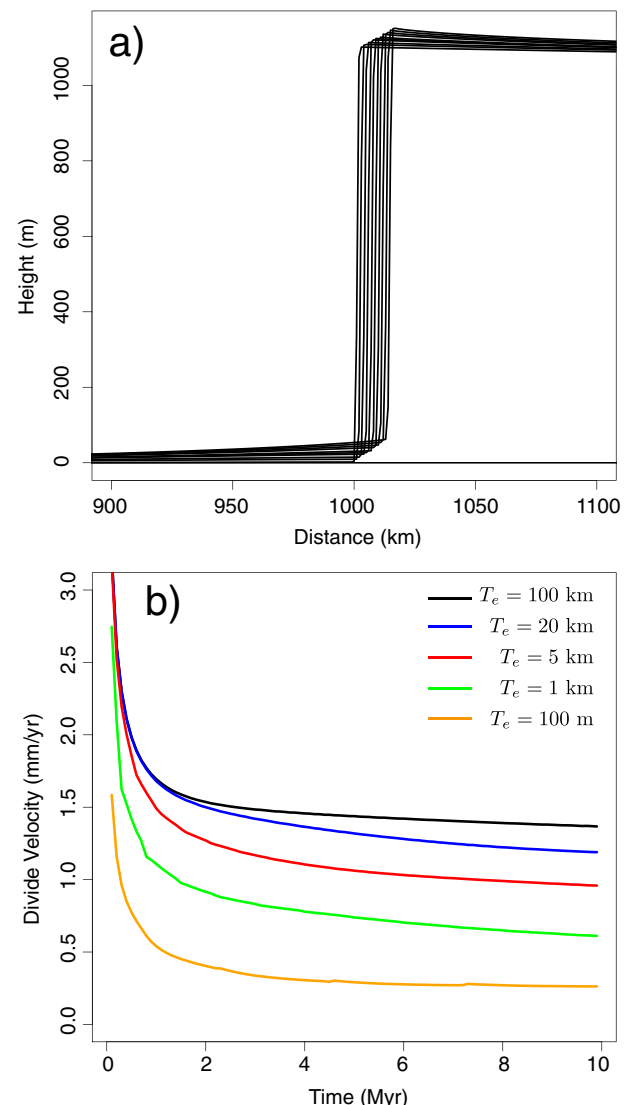


Fig. 7. a) Computed surface topography at 1 Myr intervals taking into account flexural isostatic rebound (EET = 20 km). b) Observed escarpment migration velocity for different values of the EET, T_e (see legend).

where W is the width of the escarpment. We see that for high values of D (equivalent to high values of T_e) the flexural rigidity D is very large and the isostatic factor, $\partial h / \partial E$ tends towards 1 and we recover the expression for v_d in which isostasy has been neglected (Eq. (23)). On the contrary, when the flexural rigidity is very low (equivalent to low values of T_e), the isostatic factor tends towards $1 - \rho_s / \rho_a$ or $1 - 2800 / 3150 \approx 0.1$ for the model runs presented here. This is exactly the asymptotic value towards which the escarpment velocity is tending to in the model run with $T_e = 100$ m (orange curve in Fig. 7). To further demonstrate this point, I performed another model run in which the surface density is arbitrarily set to 3149 kg/m^3 . In this case, the velocity of the divide tends towards zero (static divide). This relationship suggests therefore that the rate of escarpment retreat should also be influenced by the density of the rocks being eroded, with a higher density leading to a slower migration rate.

This final expression for the escarpment velocity (Eq. (28)) not only explains the empirical finding of Kooi and Beaumont (1994) (see their Figure 7) that the rate of escarpment retreat increases with the efficiency of both river incision (advection) and hillslope processes

(diffusion), but also scales with the effective elastic thickness of the underling lithosphere. In other words, this expression summarizes most of the major findings concerning escarpment migration velocity obtained by numerical models as summarized earlier in this review paper.

8. 2D numerical simulations

I now turn to full two-dimensional numerical experiments using the *FastScape* algorithm developed by Braun and Willett (2013). The very high efficiency of the method which is fully implicit and $O(N)$, where N is the number of nodes used to discretize the landscape, permits to reach sufficient spatial resolution to properly compute the combined effect of river incision and hillslope processes. In the following computations, we will use combinations of values of K_F , K_D and m such that the $L_E \approx 300$ m, which implies that the spatial resolution of the model must be of the order of $\Delta x = \Delta y \approx$

100 m. Such a resolution is more than an order of magnitude higher than used in any previous attempts at modeling passive margin escarpments (for example, $\Delta x = 1$ km in Kooi and Beaumont (1994) and Gilchrist et al. (1994); $\Delta x = 3$ km in Van der Beek et al. (2002); $\Delta x = 5$ km in Sacek et al. (2012)).

Using *FastScape*, we solve the two dimensional form of Eq. (5):

$$\frac{\partial h}{\partial t} = -K_F A^m \frac{\partial h}{\partial s} + K_D \left(\frac{\partial^2 h}{\partial x^2} + \frac{\partial^2 h}{\partial y^2} \right) \quad (29)$$

where A is the upstream or contributing drainage area at any point (x,y) of the landscape, and s the direction of the steepest of the eight neighbors of point (x,y) . The steepest descent algorithm (or D_8 algorithm) is also used to compute drainage direction and drainage area (Braun and Willett, 2013). To solve the diffusion term in Eq. (29), we use an Alternate Direction Implicit algorithm (ADI) and a centered finite difference approximation of the second-order derivative,

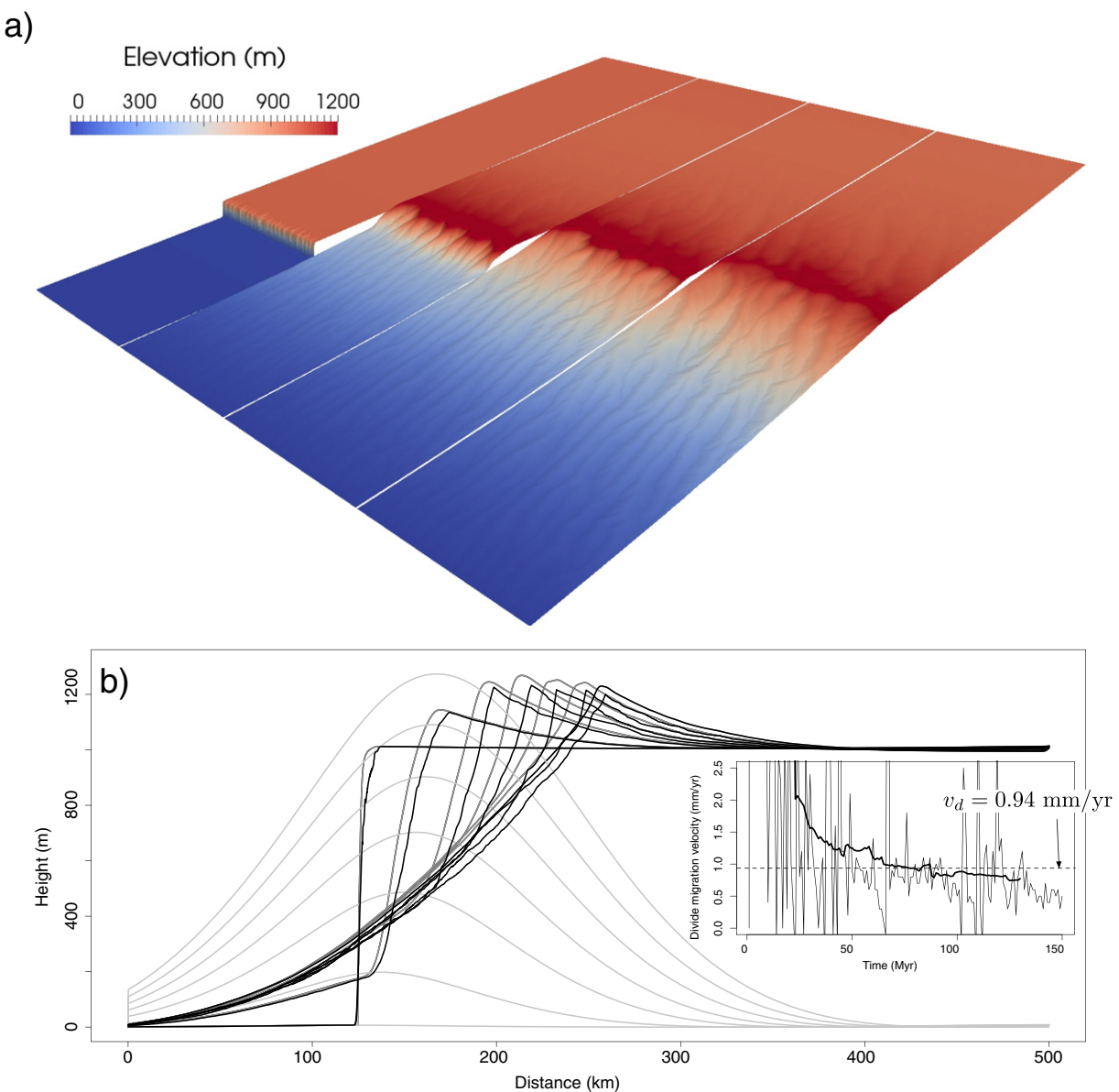


Fig. 8. a) Computed topographic elevation using the 2D landscape evolution model *FastScape* at three time steps in the model run evolution at 1, 50, 100 and 150 Myr. b) Strike (y-direction) averaged topographic profiles (black lines), maximum topographic profiles (dark grey lines) and averaged total erosion profiles (light grey lines) at times $t = 1, 25, 50, 75, 100, 125$ and 150 Myr in the model evolution. See text for model parameter values. The inset in panel b shows the observed escarpment retreat velocity as well as the intrinsic migration velocity, v_d .

which leads to an unconditionally stable and second-order accurate algorithm. The flexural isostasy equation becomes:

$$D \frac{\partial^4 \Delta u}{\partial x^4} + D \frac{\partial^4 \Delta u}{\partial x^2 \partial y^2} + D \frac{\partial^4 \Delta u}{\partial y^4} = \Delta \rho g \Delta u + \rho_s g \Delta h \quad (30)$$

and is solved by a spectral method (Nunn and Aires, 1988).

In Fig. 8 I show the results of a model run similar to the first 1D run shown in Fig. 7. The model length, L , is 500 km, its width, W , is 100 km, and it is discretized at a resolution of 100 m (5000×1000 points). The erosion parameters are $K_F = 5 \times 10^{-6} \text{ m}^{1-2m}/\text{yr}$ and $K_D = 0.14 \text{ m}^2/\text{yr}$, where $m = 0.4$. Boundary conditions are fixed elevation (base level nodes) along the top and bottom boundaries ($x = 0$ and $x = L$) and cyclic boundary conditions along the right and left boundaries ($y = 0$ and $y = W$). The initial topography is a flat, 1000 m high plateau occupying the top three quarters of the model. Flexural isostasy parameters are set to $T_e = 20 \text{ km}$, $E = 10^{11} \text{ Pa}$, $\nu = 0.25$, $\rho_s = 2800 \text{ kg/m}^3$ and $\rho_a = 3150 \text{ kg/m}^3$. Time step is 10^5 yr .

The results (Fig. 8a) show a behavior that is very similar to that predicted by the 1D model. In the earlier stages of the model run the escarpment retreats rapidly until sufficient erosion takes place to cause isostatic rebound and establish the escarpment as the main drainage divide. The escarpment then retreats at a constant velocity that tends towards an asymptotic value. In cross-section (Fig. 8b), the model evolution is almost identical to that of the 1D model (Fig. 7a), except that it has been performed for a longer period of time (150 Myr compared to 20 Myr).

In Fig. 8b I show the strike-averaged (black curves) and maximum topography (dark grey curves), as well as the strike-average total erosion (light grey curves) obtained from the 2D model run shown in panel a. The results show that, although the escarpment is the main drainage divide, it leaves in its trail a region of relatively high relief and low topography to form a gently seaward-dipping coastal plain. The total erosion increases progressively (almost linearly) with time; erosion is maximum approximately half-way between the initial and current position of the divide.

The small inset in Fig. 8b shows the computed velocity of the point of maximum y -averaged topography (thin curve) and a 20 point averaged or smoothed version of it (thick curve). This velocity can be used as a good proxy for the divide/escarpment velocity. Although relatively noisy, the curve shows a slow decrease from approximately 2 mm/yr in the early stages of evolution of the model to a relatively constant migration velocity that is very close to the theoretical, intrinsic velocity of 0.94 mm/yr obtained from Eq. (17), under the assumption

of no isostatic rebound. Assuming an escarpment half-width of 100 km, Eq. (23) predicts an intrinsic velocity of $\approx 0.7 \text{ mm/yr}$.

The model behavior can be further tested by changing several of the key parameters. In Fig. 9, I show the final computed geometry of the escarpment for five different model runs. We see that the initial height of the topography does not influence the rate of escarpment retreat. This behavior is, however, dependent on our assumption that n , the slope exponent in the stream power law, is 1. If $n \neq 1$, the topography amplitude or scaling factor h_0 cannot be simplified out to obtain the dimensionless form of the governing equation (Eq. (9)).

Decreasing the EET slows down the evolution of the escarpment, while increasing or decreasing the fluvial erosion coefficient, K_F , increases or decreases the divide/escarpment migration velocity, in accordance with theoretical predictions (Eq. (23)).

9. Future work

The present-day rate of erosion at and around passive margin escarpments, as determined by cosmogenic nuclide analysis, is very low, i.e. of the order of a few meters to tens of meters per Myr. This usually contrasts with the mean retreat rate of 1 km/Myr that can be derived from the ratio of the present-day position of the escarpment from the coastline by the time since rifting or breakup. In all of the model runs presented here and/or in previous modeling studies of passive margin escarpments, escarpment retreat rates are very steady, apart for a period of apparent rapid migration in the early stages of most model runs. That early stage corresponds to the relaxation of the imposed initial geometry and may be difficult to relate to a natural process.

This means that we have not yet found a clear process by which an escarpment could change its migration velocity. One potential solution that has been proposed by several authors (Brown et al., 2002; Cockburn et al., 2000a; Fleming et al., 1999) is that, prior to rifting, there existed an inland continental divide that is not the escarpment. The initial escarpment rapidly degrades until the area between the coastline and the pre-existing divide is eroded away. A new escarpment then forms at the position of the pre-existing divide. This so-called “plateau degradation or downwearing” scenario is illustrated in Fig. 3b. It explains why present-day escarpment erosion rates and retreat rates are apparently very low despite the apparently large distance separating them from their “original” position.

It is, however, interesting to compare escarpment retreat rates computed in our models with the local erosion rates predicted near the escarpment. In Fig. 10, we show the computed erosion rates at

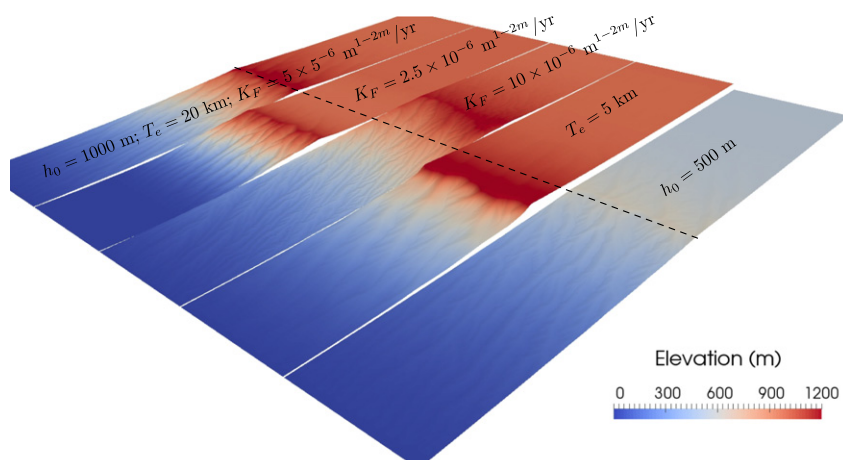


Fig. 9. Final escarpment geometry (i.e. at $t = 150 \text{ Myr}$) for five model runs (from top left to bottom right): reference model (as shown in Fig. 8a), reduced fluvial erosion, enhanced fluvial erosion, reduced EET and reduced initial topographic height. The dashed line shows the predicted position of the divide in the reference run.

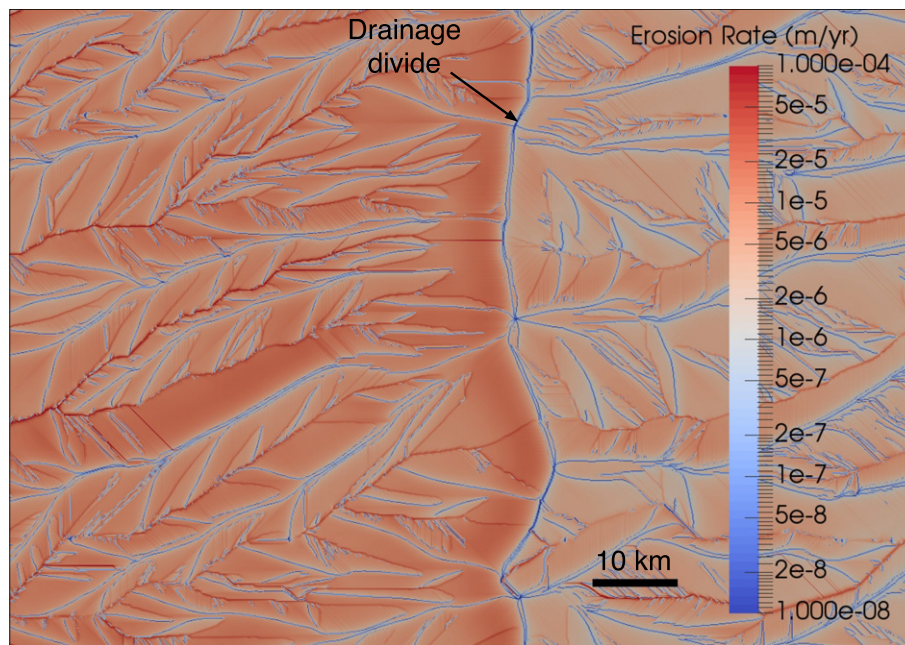


Fig. 10. Predicted erosion rate in the final time step of the reference model run (Fig. 8a) and in the vicinity of the escarpment top, which is also the drainage divide. Values at the divide itself are as low as 10^{-8} m/yr and do not exceed $1\text{--}5 \times 10^{-5}$ m/yr, i.e. 10 to 50 m/Myr, in the adjacent areas. Despite these low local erosion rates, the divide is migrating to the right at a velocity of 1 km/Myr.

the final time step (i.e. 150 Myr in its evolution) for the reference model shown in Fig. 8a. The predicted escarpment retreat rate is approximately 1 km/Myr. It explains the final position of the escarpment approximately 150 km from the original coastline without requiring any recent slowdown in escarpment retreat rate. Computed erosion rate in the vicinity of the escarpment is markedly lower than the escarpment/divide migration rate. It is approximately $2\text{--}5 \times 10^{-5}$ m/yr or 20–50 m/Myr along the hillslopes on either sides of the divide (light to dark red areas within a few kilometers form the main divide). It is approximately nil at the divide itself. The largest values (1×10^{-4} m/yr or 100 m/Myr) are predicted in the streams on either sides of the divide. Note that these predictions are only made possible by the high spatial resolution of our model (100 m grid spacing). These model results suggest that the low erosion rate observed around escarpments do not necessarily mean that the escarpment is moving at a slower rate today than in the past. An expression similar to Eq. (14), relating escarpment retreat rate to local erosion rate, is needed to make full use of the information derived from cosmogenic isotope studies. More generally, further modeling and an improved quantitative estimate of escarpment/divide migration rate as derived from estimates of erosion rate in the vicinity of the escarpment are required.

10. Summary of findings

I have derived and presented a new expression for the migration or retreat velocity of a drainage divide. Using 1D and 2D landscape evolution models solving the basic geomorphic equations that describe the balance between fluvial incision and hillslope processes, I have demonstrated the validity of this expression, which explains the dependence of escarpment retreat rate on the value of the rate parameters in the governing equation, namely K_F and K_D . I have also shown and explained why flexural isostasy can change the escarpment retreat velocity and that is controlled by the assume effective elastic thickness but also by the density of rocks being eroded during the migration of the escarpment.

I have also shown that great caution should be exerted to derive past or present-day rates of escarpment migration from thermochronological data and cosmogenic nuclide studies. Using a high resolution LEM, I have shown that rates of erosion near or at a passive margin escarpment can be several orders of magnitude smaller than the escarpment migration velocity. This finding may explain the large differences between observed present-day escarpment retreat rates and long-term estimates derived from their position from the coastline.

Acknowledgments

This research did not receive any specific grant from funding agencies in the public, commercial, or not-for-profit sectors. The author thanks Sean Willett for a very insightful review that helped improve an earlier version of this manuscript and, in particular, for suggesting Eq. (14) that helped in the interpretation of the modeling results. Rod Brown also provided useful comments and suggestions on an earlier version of this manuscript. Some of the work presented here was accomplished while J. B. was at the Earth and Planetary Sciences Department, University of California, Berkeley, USA.

Appendix A. Supplementary data

Supplementary data to this article can be found online at <http://dx.doi.org/10.1016/j.gr.2017.04.012>.

References

- Beauvais, A., Bonnet, N.J., Chardon, D., Arnaud, N., Jayananda, M., 2016. Very long-term stability of passive margin escarpment constrained by $^{40}\text{Ar}/^{39}\text{Ar}$ dating of K-Mn oxides. *Geology* 44, 299–302.
- Braun, J., Beaumont, C., 1989. A physical explanation of the relation between flank uplifts and the breakup unconformity at rifted continental margins. *Geology* 17, 760–764.

- Braun, J., Deschamps, F., Rouby, D., Dauteuil, O., 2012. Flexure of the lithosphere and the geodynamical evolution of non-cylindrical rifted passive margins: results from a numerical model incorporating variable elastic thickness, surface processes and 3D thermal subsidence. *Tectonophysics* 604, 1–11.
- Braun, J., Guillocheau, F., Robin, C., Baby, G., Jelsma, H., 2014. Rapid erosion of the Southern African plateau as it climbs over a mantle superswell. *Journal of Geophysical Research* 119, 6093–6112.
- Braun, J., Simon-Labrec, T., Murray, K.E., Reiners, P.W., 2014. Topographic relief driven by variations in surface rock density. *Nature Geoscience* 7, 534–540.
- Braun, J., van der Beek, P., 2004. Evolution of passive margin escarpments: what can we learn from low-temperature thermochronology. *Journal of Geophysical Research* 109, F04009. <http://dx.doi.org/10.1029/2004JF000147>.
- Braun, J., Willett, S., 2013. A very efficient $O(n)$, implicit and parallel method to solve the basic stream power law equation governing fluvial incision and landscape evolution. *Geomorphology* 180–181, 170–179.
- Brown, R., Rust, D., Summerfield, M., Gleadow, A., de Wit, M., 1990. An Early Cretaceous phase of accelerated erosion on the south-western margin of Africa: evidence from apatite fission track analysis and the offshore sedimentary record. *Nuclear Tracks and Radiation Measurements* 17, 339–350.
- Brown, R., Summerfield, M., Gleadow, A., 2002. Denudational history along a transect across the Drakensberg Escarpment of southern Africa derived from apatite fission track thermochronology. *Journal of Geophysical Research* 107, 2350. <http://dx.doi.org/10.1029/2001JB000745>.
- Buck, W., 1986. Small-scale convection induced by passive rifting: the cause for uplift of rift shoulders. *Earth and Planetary Science Letters* 77, 362–372.
- Campanile, D., Nambiar, C.G., Bishop, P., Widdowson, M., Brown, R., 2008. Sedimentation record in the Konkan-Kerala basin: implications for the evolution of the Western Ghats and the Western Indian passive margin. *Basin Research* 20 (1), 3–22.
- Cochran, J., 1983. Effects of finite extension times on the development of sedimentary basins. *Earth and Planetary Science Letters* 66, 289–302.
- Cockburn, H., Brown, R., Summerfield, M., Seidl, M., 2000. Quantifying passive margin denudation and landscape development using a combined fission-track thermochronology and cosmogenic isotope analysis approach. *Earth and Planetary Science Letters* 179 (3–4), 429–435.
- Cockburn, H., Brown, R., Summerfield, M., Seidl, M., 2000. Quantifying passive margin denudation and landscape development using combined fission-track thermochronology and cosmogenic isotope analysis. *Earth and Planetary Science Letters* 179, 429–435.
- Fleming, A., Summerfield, M., Stone, J., Fifield, L., Creswell, R., 1999. Denudation rates for the southern Drakensberg escarpment, SE Africa, derived from in-situ-produced cosmogenic ^{36}Cl : initial results. *Journal of the Geological Society of London* 156, 209–212.
- Gallagher, K., Hawkesworth, C., Mantovani, M., 1994. The denudation history of the onshore continental margin of SE Brazil inferred from apatite fission track data. *Journal of Geophysical Research* 99, 18117–18145.
- Gilchrist, A., Kooi, H., Beaumont, C., 1994. Post-Gondwana geomorphic evolution of southeastern Africa: implications for the controls on landscape development from observations and numerical experiments. *Journal of Geophysical Research* 99, 12221–12228.
- Gilchrist, A., Summerfield, M., 1990. Differential denudation and flexural isostasy in formation of rifted-margin upwarps. *Nature* 346, 739–742.
- Guillocheau, F., Rouby, D., Robin, C., Helm, C., Rolland, N., Le Carlier de Veslud, C., Braun, J., 2012. Quantification and causes of the terrigenous sediment budget at the scale of a continental margin: a new method applied to the Namibia-South Africa margin. *Basin Research* 24, 3–30.
- Gunnell, Y., Fleitout, L., 1998. Shoulder uplift of the Western Ghats passive margin, India: a denudational model. *Earth Surface Processes and Landforms* 23 (5), 391–404.
- Gunnell, Y., Harbor, D.J., 2010. Butte detachment: how pre-rift geological structure and drainage integration drive escarpment evolution at rifted continental margins. *Earth Surface Processes and Landforms* 35 (12), 1373–1385.
- Heimstra, A.M., Chappell, J., Finkel, R.C., Fifield, K., Alimanovic, A., 2006. Escarpment erosion and landscape evolution in southeastern Australia. Special Paper 398: Tectonics, Climate, and Landscape Evolution. Geological Society of America, pp. 173–190.
- Japsen, P., Chalmers, J.A., Green, P.F., Bonow, J.M., 2012. Elevated, passive continental margins: not rift shoulders, but expressions of episodic, post-rift burial and exhumation. *Global and Planetary Change* 90–91 (C), 73–86.
- Keen, C., 1985. The dynamics of rifting: deformation of the lithosphere by active and passive driving mechanisms. *Geophysical Journal of the Royal Astronomical Society* 80, 95–120.
- Kooi, H., Beaumont, C., 1994. Escarpment evolution on high-elevation rifted margins: insights derived from a surface processes model that combines diffusion, advection and reaction. *Journal of Geophysical Research* 99, 12191–12209.
- Kounov, A., Niedermann, S., de Wit, M., Viola, G., Andreoli, M., Erzinger, J., 2007. Present denudation rates at selected sections of the South African escarpment and the elevated continental interior based on cosmogenic ^{3}He and ^{21}Ne . *South African Journal of Geology* 110, 235–248.
- Lidmar-Bergstrom, K., Ollier, C., Sulebak, J., 2000. Landforms and uplift history of southern Norway. *Global and Planetary Change* 24, 211–231.
- Lister, G., Etheridge, M., Symonds, P., 1991. Detachment models for the formation of passive continental margins. *Tectonics* 10, 211–231.
- Mandal, S.K., Lupker, M., Burg, J.-P., Valla, P.G., Haghipour, N., Christl, M., 2015. Spatial variability of ^{10}Be -derived erosion rates across the southern Peninsular Indian escarpment: a key to landscape evolution across passive margins. *Earth and Planetary Science Letters* 425, 154–167.
- Matmon, A., Bierman, P., Enzel, Y., 2002. Pattern and tempo of great escarpment erosion. *Geology* 30, 1135–1138.
- Montgomery, D., 2001. Slope distributions, threshold hillslopes, and steady-state topography. *American Journal of Science* 301, 432–454.
- Nunn, J., Aires, J., 1988. Gravity anomalies and flexure of the lithosphere at the middle Amazon basin, Brazil. *Journal of Geophysical Research* 93, 415–428.
- Perron, J., Dietrich, W., Kirchner, J., 2008. Controls on the spacing of first-order valleys. *Journal of Geophysical Research* 113, F04016.
- Petit, C., Fournier, M., Gunnell, Y., 2007. Tectonic and climatic controls on rift escarpments: erosion and flexural rebound of the Dhofar passive margin (Gulf of Aden, Oman). *Journal of Geophysical Research* 112 (B3), B03406–B03415.
- Peulvast, J.-P., Claudino Sales, V., Bétard, F., Gunnell, Y., 2008. Low post-Cenomanian denudation depths across the Brazilian Northeast: implications for long-term landscape evolution at a transform continental margin. *Global and Planetary Change* 62 (1–2), 39–60.
- Press, W., Teukolky, S., Vetterling, W., Flannery, B., 1992. Numerical Recipes, the Art of Scientific Computing. First edition, Cambridge University Press, Cambridge, England.
- Rouby, D., Bonnet, S., Guillocheau, F., Braun, J., Biancotto, F., Robin, C., Dauteuil, O., Gallagher, K., 2009. Sediment supply to the Orange sedimentary system over the last 150 Ma: an evaluation from erosion/sedimentation balance. *Marine and Petroleum Geology* 26, 782–794.
- Royden, L., Keen, C., 1980. Rifting process and thermal evolution of the continental margin of eastern Canada determined from subsidence curves. *Earth and Planetary Science Letters* 51, 343–361.
- Sacek, V., Braun, J., Van der Beek, P., 2012. The influence of rifting on escarpment migration on high elevation passive continental margins. *Journal of Geophysical Research* 117 (B4), B04407.
- Seidl, M., Weissel, J., Pratson, L., 1996. The kinematics and pattern of escarpment retreat across the rifted continental margin of SE Australia. *Basin Research* 12, 301–316.
- Steer, P., Huismans, R.S., Valla, P., Gac, S., Herman, F., 2012. Bimodal Plio-Quaternary glacial erosion of fjords and low-relief surfaces in Scandinavia. *Nature Geoscience* 5, 635–639.
- Sugden, D., Denton, G., 2004. Cenozoic landscape evolution of the Convoy Range to Mackay Glacier area, transantarctic mountains: onshore to offshore synthesis. *Geological Society of America Bulletin* 116, 840–857.
- Summerfield, M., 2005. A tale of two scales, or the two geomorphologies. *Transactions of the Institute of British Geographers* 30, 402–405.
- Torsvik, T., Rousse, S., Labails, C., Smethurst, M., 2009. A new scheme for the opening of the South Atlantic Ocean and the discussion of an Aptian salt basin. *Geophysical Journal International* 1315–1333.
- Tucker, G., Slingerland, R., 1994. Erosional dynamics, flexural isostacy, and long-lived escarpments: a numerical modeling study. *Journal of Geophysical Research* 99, 12229–12243.
- Turcotte, D., Schubert, G., 1982. Geodynamics: Applications of Continuum Physics to Geological Problems. First edition, John Wiley and Sons, New York.
- Van Balen, R., van der Beek, P., Cloetingh, S., 1995. The effect of rift shoulder erosion on stratigraphic patterns at passive margins: implications for sequence stratigraphy. *Earth and Planetary Science Letters* 134 (3–4), 527–544.
- Van der Beek, P., Andriessen, P., Cloetingh, S., 1995. Inferences from a coupled tectonic-surface processes. *Tectonics*.
- Van der Beek, P., Braun, J., 1998. Numerical modelling of landscape evolution on geological time scales: a parameter analysis and comparison with the southeastern highlands of Australia. *Basin Research* 10, 49–68.
- Van der Beek, P., Braun, J., 1999. Controls on post-mid-Cretaceous landscape evolution in the southeastern highlands of Australia: insights from numerical surface process models. *Journal of Geophysical Research* 104, 4945–4966.
- Van der Beek, P., Braun, J., Lambeck, K., 1999. Post-palaeozoic uplift history of southeastern Australia revisited: results from a process-based model of landscape evolution. *Australian Journal of Earth Sciences* 46, 157–172.
- Van der Beek, P., Pulford, A., Braun, J., 2001a. Cenozoic landscape development in the Blue Mountains (SE Australia): lithological and tectonic controls on rifted margin morphology. *Journal of Geology*.
- Van der Beek, P., Pulford, A., Braun, J., 2001b. Cenozoic landscape evolution in the Blue Mountains (SE Australia): lithological and tectonic controls on rifted margin morphology. *Journal of Geology* 109, 35–56.
- Van der Beek, P., Summerfield, M., Braun, J., Brown, R., Fleming, A., 2002. Modelling post-breakup landscape development and denudational history across the southeast African (Drakensberg escarpment) margin. *Journal of Geophysical Research* 107, 2351. <http://dx.doi.org/10.1029/2001JB000744>.
- Van Der Beek, P., Summerfield, M.A., Braun, J., Brown, R.W., Fleming, A., 2002. Modeling postbreakup landscape development and denudational history across the southeast African (Drakensberg escarpment) margin. *Journal of Geophysical Research* 107 (B12), 2351.
- Vanacker, V., von Blanckenburg, F., Hewawasam, T., Kubik, P., 2007. Constraining landscape development of the Sri Lankan escarpment with cosmogenic nuclides in river sediments. *Earth and Planetary Science Letters* 253, 402–414.
- Walford, H., White, N., 2005. Constraining uplift and denudation of west African continental margin by inversion of stacking velocity data. *Journal of Geophysical Research* 110.
- Weissel, J., Karner, G., 1989. Flexural uplift of rift flanks due to mechanical unloading of the lithosphere during extension. *Journal of Geophysical Research* 94, 13919–13950.
- Weissel, J., Seidl, M., 1997. Influence of rock strength properties on escarpment retreat across passive continental margins. *Geology* 25, 631–634.

- Weissel, J., Seidl, M., 1998. Inland propagation of erosional escarpments and river profile evolution across the southeast Australian passive continental margin. In: Tinkler, K.J., Wohl, E.E. (Eds.), *Rivers Over Rock: Fluvial Processes in Bedrock Channels*. 107. American Geophysical Union, pp. 189–206.
- Wildman, M., Brown, R., Beucher, R., Persano, C., Stuart, F., Gallagher, K., Schwanethal, J., Carter, A., 2016. The chronology and tectonic style of landscape evolution along the elevated Atlantic continental margin of South Africa resolved by joint apatite fission track and (U-Th-Sm)/He thermochronology. *Tectonics* 35, 511–545.
- Wildman, M., Brown, R., Watkins, R., Carter, A., Gleadow, A., Summerfield, M., 2015. Post break-up tectonic inversion across the southwestern cape of South Africa: new insights from apatite and zircon fission track thermochronometry. *Tectonophysics* 654, 30–55.
- Willgoose, G., Bras, R., Rodriguez-Iturbe, I., 1991. A physically based coupled network growth and hillslope evolution model: 1. Theory. *Water Resources Research* 27, 1671–1684.



Jean Braun is a Senior Scientist at the German Research Center for Geosciences (GFZ) in Potsdam, Germany and a Professor at the University of Potsdam. He is a Scientific Editor for *Terra Nova*, author of over 120 publications in peer-reviewed journals and of a textbook on Quantitative Thermochronology. His current research interests include modeling Earth surface processes and their interactions with the solid Earth and the hydrosphere.